Using In-situ Wettability Measurements to Reconstruct the Wetting Condition of a Natural Rock

Ruichang Guo[1], Laura E. Dalton[2], Hongsheng Wang[1], James McClure[1], Dustin Crandall[2], Cheng Chen[3]

[1] VIRGINIA TECH
[2] NATIONAL ENERGY TECHNOLOGY LABORATORY
[3] STEVENS INSTITUTE OF TECHNOLOGY

MAY 30, 2022

Outline

1. Objective
2. Review on wettability heterogeneity model
3. Modeling and reconstructing heterogeneous wettability
4. Implications on immiscible displacement
5. Summary

1. Objective

- In-situ measurements of wettability on natural rocks published recently suggest that wettability heterogeneity of a natural rock is at a subpore scale and wettability has a wide range.
- This work is to model the heterogeneous wettability based on in-situ wettability measurements on a Bentheimer sandstone and explore the implications of pore-scale wettability heterogeneity on immiscible displacement in a sandstone.

2. Review on Wettability Heterogeneity Model

Literature review on wettability heterogeneity model of a porous medium

Studies	Porous media	Fluids	Methods	Surface wettability
(Bakhshian and Hosseini 2019)	Tuscaloosa sandstone	Brine/CO_2	LB modeling	Fractional wet
(Maziar Arshadi 2020)	Arkose	N/A[1]	Experiment and pore network modeling	Fractional wet
(Zhao et al. 2018)	Computer-generated solid spheres	N/A	LB modeling	Fractional wet
(Landry et al. 2014)	Glass and polyethylene bead packs	Brine/kerosene	Experiment and LB modeling	Mixed wet
(Hwang et al. 2006)	Mixture of quartz sand and organosilane-treated sand	Water/oil	Experiment	Fractional wet
(Masalmeh 2003)	Carbonate	Water/oil	Experiment	Mixed wet
(Bradford and Leij 1995)	Mixture of octadecyltrichlorosilane-treated and untreated sands	Water/air, water/oil, and water/ail/oil	Experiment	Fractional wet

Mixed wet

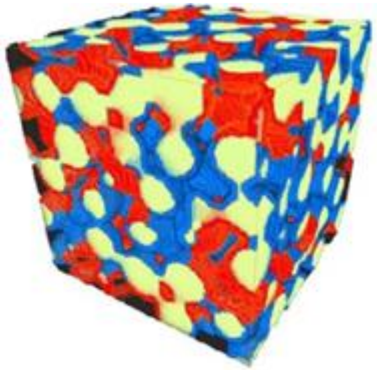

Solid

Water wet surface

Non-water wet surface

(Landry et al, WRR,2014)

Fractional wet

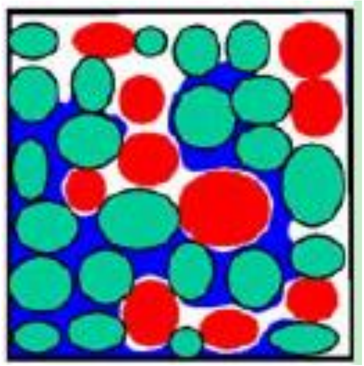

Water-wet grains

Non-water- wet grains

Water

Air

(Hwang et al. AWR, 2006)

Fractional wet

Water-wet

Non-water-wet

Pore space

(Bakhshian et al,AWR, 2019)

3. Modeling Wettability Heterogeneity

3.1 In-situ measurements of wettability

- The core flooding experiment and X-ray micro-CT imaging were performed at U.S. Department of Energy (DOE)'s National Energy Technology Laboratory (NETL).

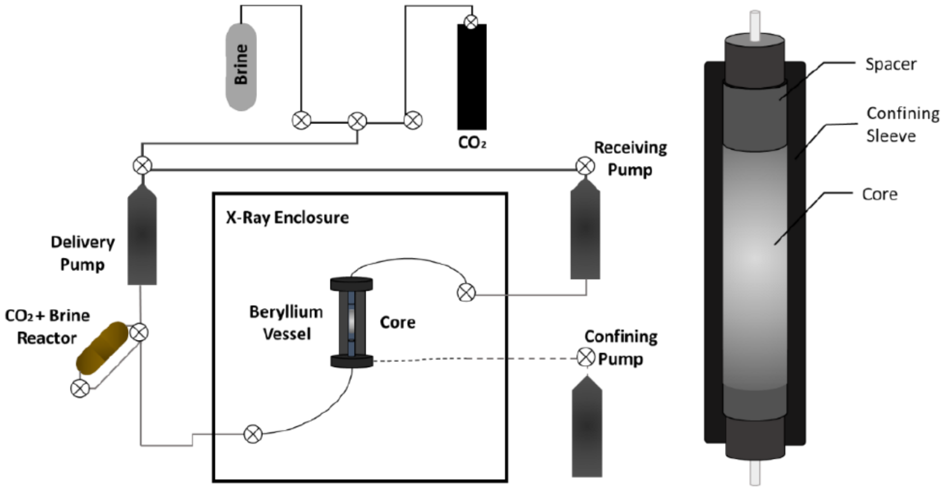

Core flooding experiment setup

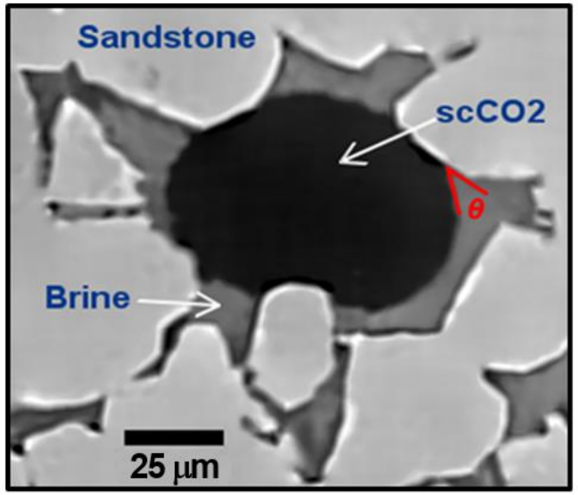

Schematic diagram on contace angle measurement

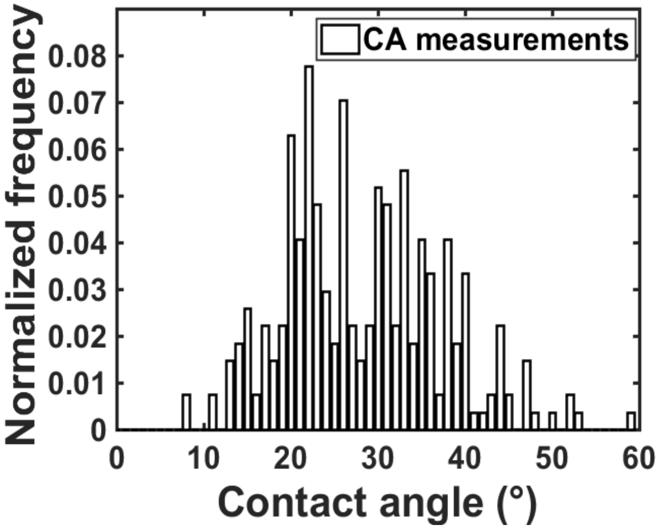

Distribution of contact angles

3. Modeling Wettability Heterogeneity

3.2 Model heterogeneous wettability as a random field

Model

Distribution model: Lognormal

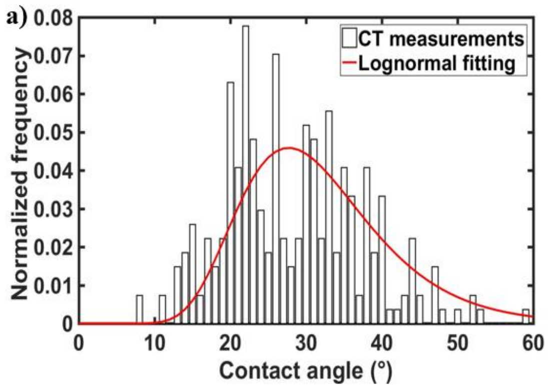

Correlation

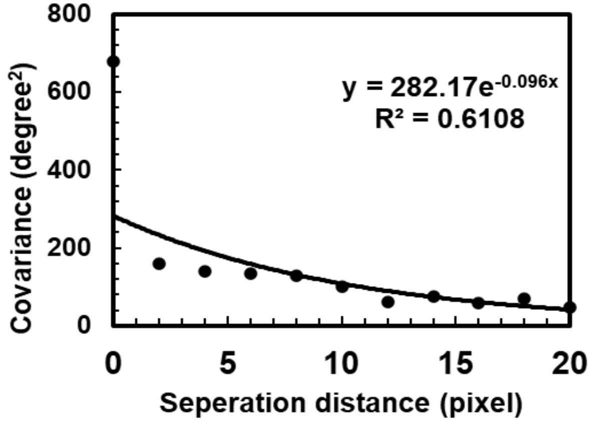

Generation

Lognormal assumption:

$$Y \sim N(\mu_Y, \sigma_Y^2) \qquad Y = \log(\theta)$$

Correlation matrix decomposition:

$$c_Y(\mathbf{x},\mathbf{y}) = \sigma_Y^2 \exp\left[-\left(|x_1 - y_1|/L_1 + |x_2 - y_2|/L_2 + |x_3 - y_3|/L_3\right)\right]$$

$$c_Y(\mathbf{x},\mathbf{y}) = \sum_{n=1}^{\infty} \lambda_n \psi_n(\mathbf{x}) \psi_n(\mathbf{y})$$

Generate Y field:

$$\mathbf{Y}(\mathbf{x}) = \langle \mathbf{Y}(\mathbf{x}) \rangle + \sum_{n=1}^{\infty} \xi_n \sqrt{\lambda_n} \psi_n(\mathbf{x})$$

Karhunen-Loève expansion

Wettability construction

- Convert the Y field into a θ field
- Mapping the θ field onto the Bentheimer sandstone

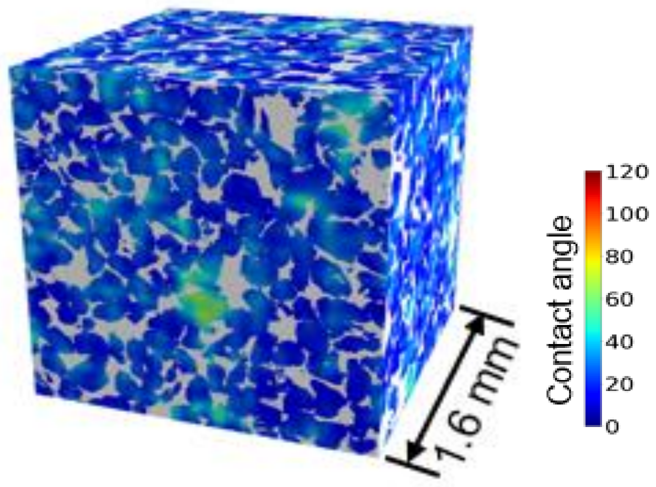

3. Modeling Wettability Heterogeneity

3.3 Reconstruction of heterogeneous wettability

Wettability Field Generation **Reconstruction**

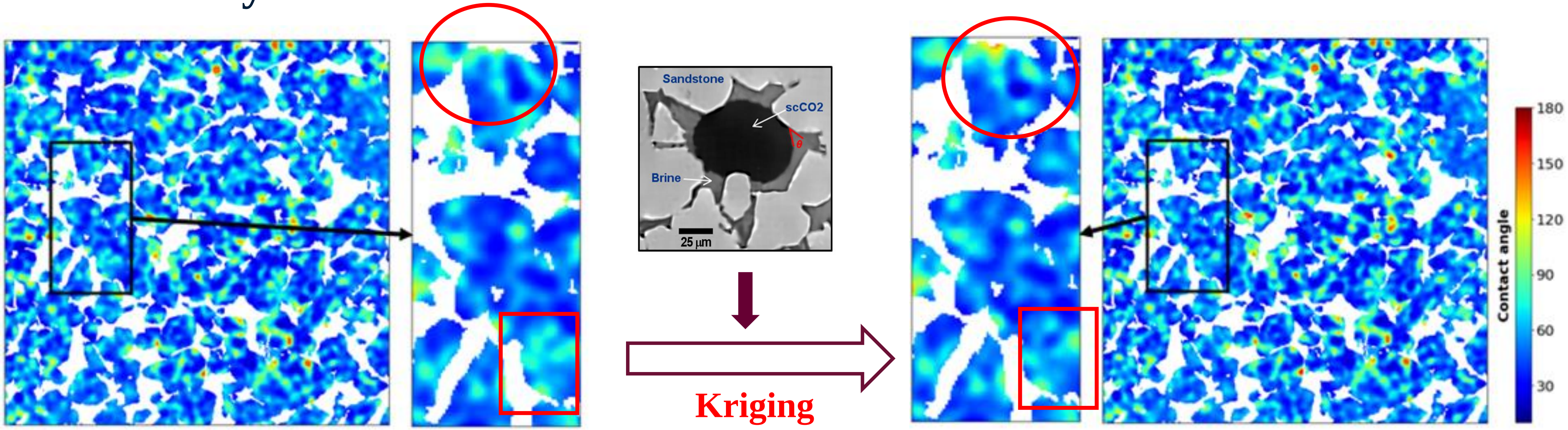

Wettability field generation

Conditioned wettability field with measured CAs

$$Y_{cs}(\mathbf{x}) = Y_{us}(\mathbf{x}) + Y_{SK}(\mathbf{x}) - Y_{SK,us}(\mathbf{x})$$

Y_{cs} Conditional wettability field

Y_{us} Unconditional wettability

Y_{SK} Wettability field kriged from measured wettability

$Y_{SK,us}$ Wettability kriged from simulated wettability

4. Implications on immiscible displacements in porous media

4.1 Generated hterogeneous wettability models

The investigations were conducted in the context of geological carbon sequestration.

Wettability classification in a CO_2-Brine-Rock system

Strongly water-wet	Weakly water-wet	Intermeidate wet	Weakly CO_2 -wet	Strongly CO_2-wet

0° 50° 70° 110° 130° 180°

(Iglauer et al., 2015)

Wettability field generation

- Method: Karhunen-Loève expansion （KLE）
- Stotistical parameters： Standard deviation, 9°
  Correlation length, 118.6 μm

Direct simulation

- Color-gradient LB multiphase model
- Hybrid, multicore CPU/GPU parallel computing

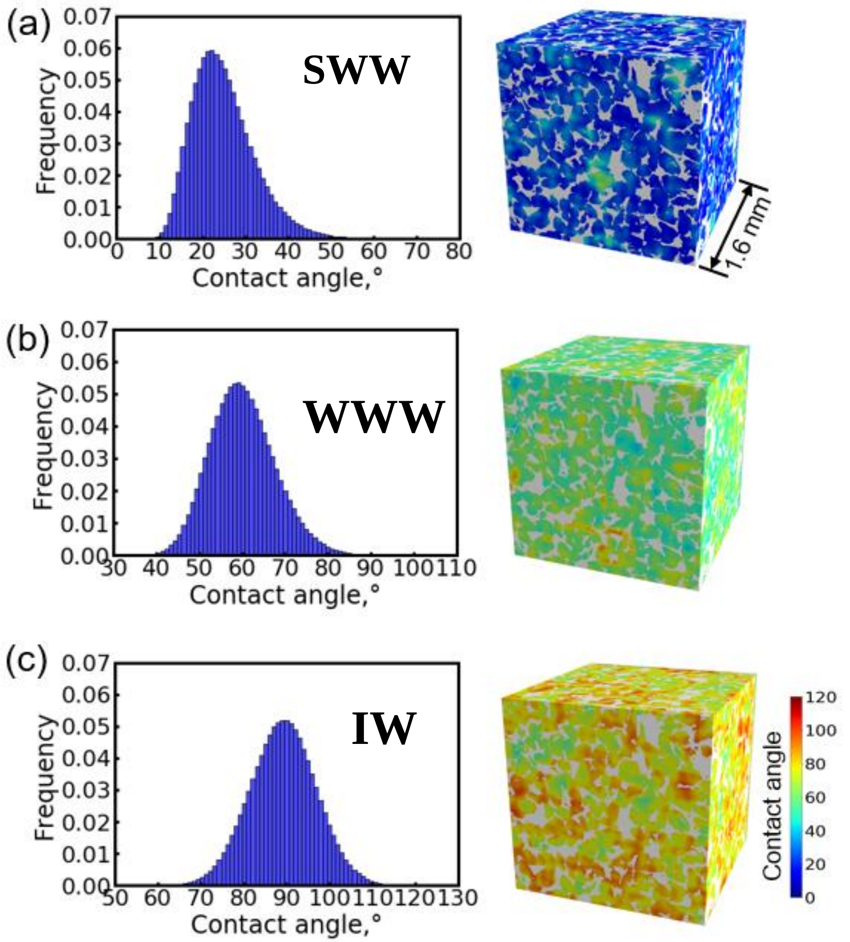

VIRGINIA TECH

4. Implications on immiscible displacements in porous media

4.2 Impact on $scCO_2$/water configuration

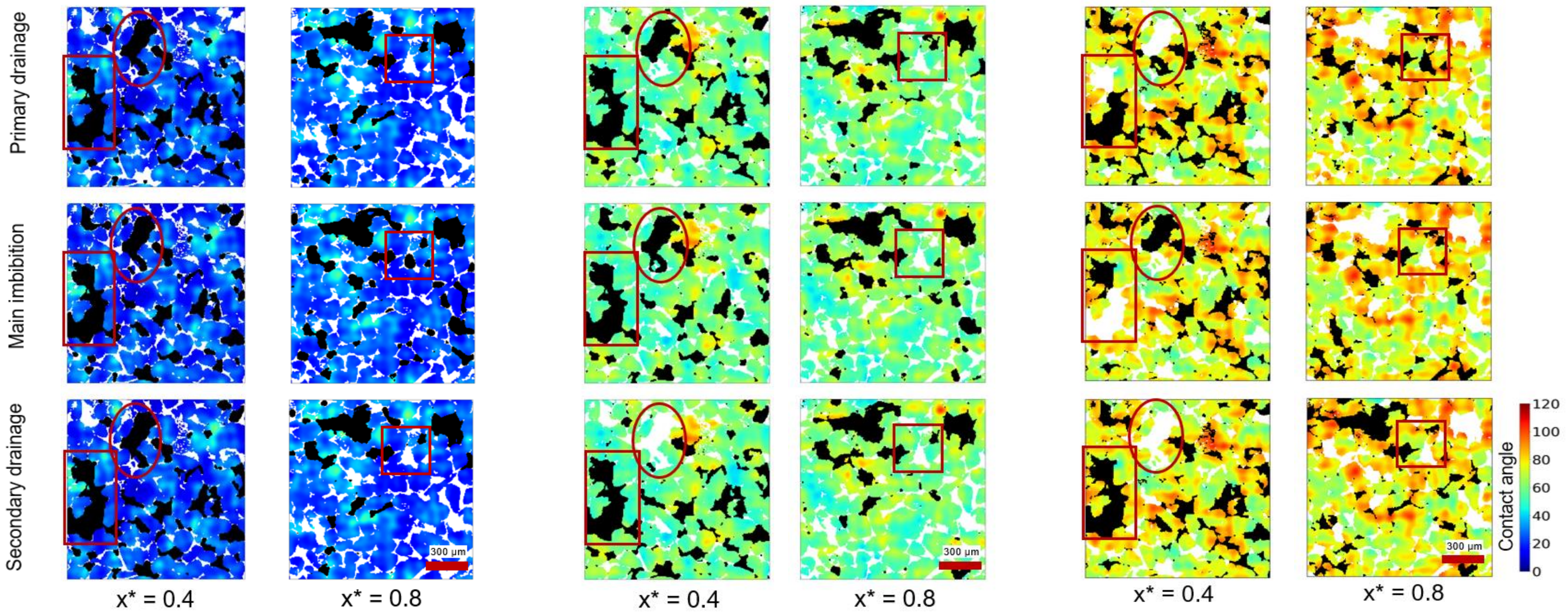

Strongly water-wet condition, Sw = 0.5 Weakly water-wet condition, Sw = 0.5 Intermediate wet condition, Sw = 0.5

4. Implications on immiscible displacements in porous media

4.3 Impact on Pc-Sw curve

- The *Pc*-*Sw* curves for homogeneous and heterogeneous wetting condition are consistent.
- Pore-scale heterogeneity effects on local redistribution of $scCO_2$/water plumes are averaged out on macroscopic *PC*-*Sw* curve.
- Under homogeneous IW condition, the entry pressure for PD path is zero;
- Under heterogeneous IW condition, the entry pressure for PD path is negative.

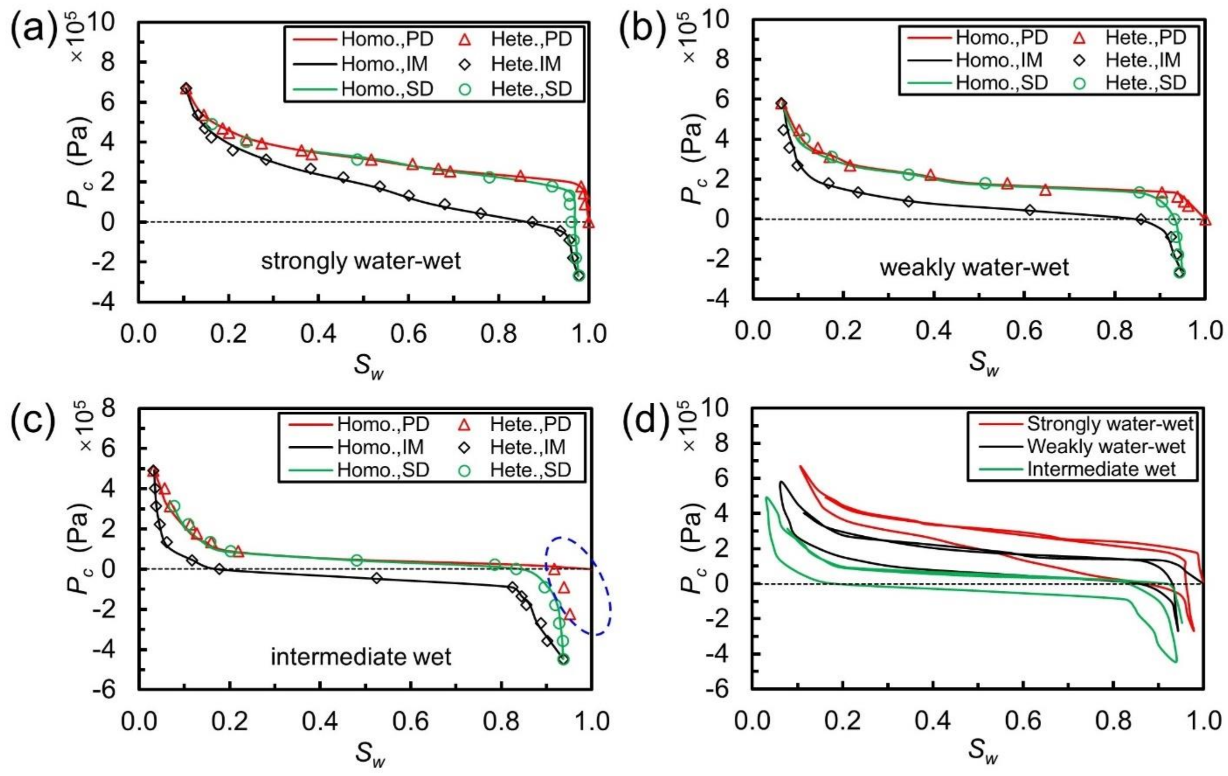

To ensure the accuracy, enough timesteps are simulated. The average total time step for each case is 3.12×10^8.

4. Implications on immiscible displacements in porous media

4.4 Impact on relative permeability

Heterogeneous

Homogeneous

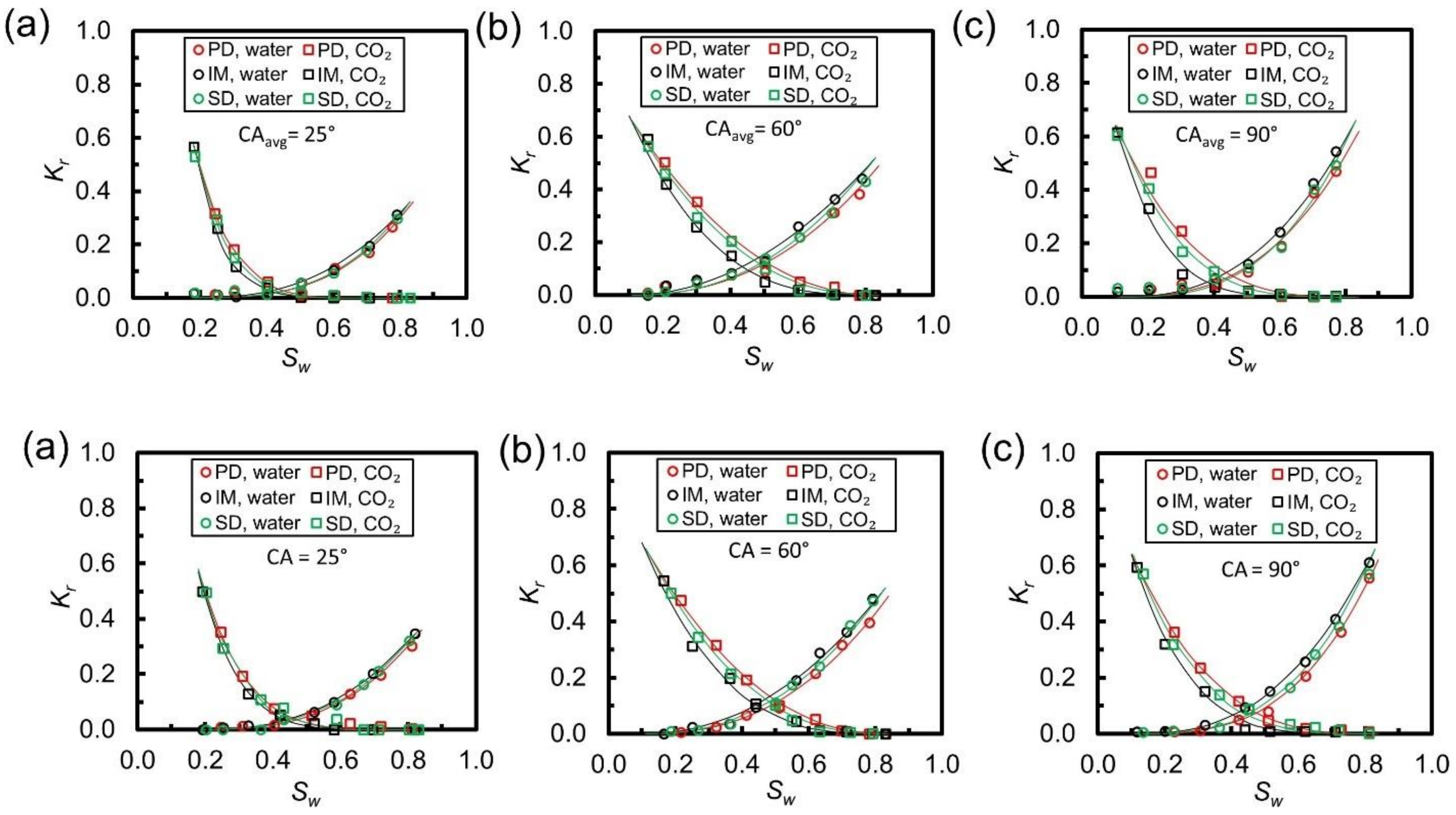

Relative permeabilities under heterogeneous and homogeneous wettabiltiy

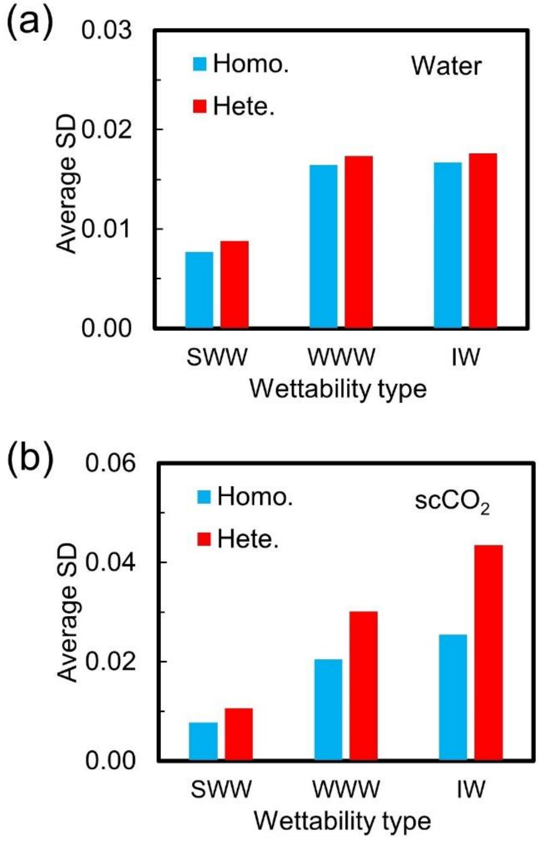

Uncertainty caused by wettability heterogeneity

5. Summary

❑ Summary

- ❑ In-situ measurements of wettability confirmed that wettability of a natural rock was heterogeneous at a subpore scale. The wettability followed a lognormal distribution.
- ❑ Pore-scale wettability heterogeneity does not cause noticeable impact on *Pc*-*Sw* curve, except that under the heterogeneous IW condition, the entry pressure of the PD stage was negative, whereas it was zero under the homogeneous IW condition.
- ❑ Pore-scale wettability heterogeneity causes noticeable uncertainty in relative permeabilities.

❑ Acknowlegements

❑ The authors are thankful to the financial support provided by the U.S. Department of Energy (DOE)'s National Energy Technology Laboratory (NETL), and the support of supercomputers from Virginia Tech's Advanced Research Computing.

❑ Reference

- Bakhshian, S. and S. A. Hosseini (2019). Pore-scale analysis of supercritical CO_2-brine immiscible displacement under fractional-wettability conditions. Advances in Water Resources, 126: 96-107.
- Guo, R., et al. (2020). The role of the spatial heterogeneity and correlation length of surface wettability on two-phase flow in a CO_2-water-rock system. Advances in Water Resources, 146.
- Guo, R., et al. (2022). Role of heterogeneous surface wettability on immiscible displacement, capillary pressure, and relative permeability in a CO2-brine-rock system. Advances in Water Resources, in press.
- Hwang, S. I., et al. (2006). Effects of fractional wettability on capillary pressure-saturation-relative permeability relations of two-fluid systems. Advances in Water Resources, 29: 212-226.
- Iglauer, S., et al. (2015). CO2 wettability of seal and reservoir rocks and the implications for carbon geo-sequestration. Water Resources Research, 51: 729-774.
- Landry, C. J., et al. (2014). Relative permeability of homogenous-wet and mixed-wet porous media as determined by pore-scale lattice Boltzmann modeling. Water Resources Research, 50: 3672-3689.

Thank you!

Appendix： The impact of pore-scale wettability heterogeneity on relative permeability

❑ Research plan

Comprehensive sensitivity analysis to study the respective and combined effects of standard deviation and correlation length of surface CAs.

μ_Y = 3.3623, σ_Y= 0.1000; μ_θ= 29°; σ_θ = 2°; L = 35 pixels	μ_Y = 3.3213, σ_Y= 0.3033; μ_θ= 29°, σ_θ = 9°; L = 35 pixels	μ_Y= 3.2044; σ_Y= 0.5709 μ_θ= 29°, σ_θ = 18°; L = 35 pixels
μ_Y= 3.3623, σ_Y=0.1000; μ_θ= 29 °, σ_θ = 2°; L = 71 pixels	μ_Y= 3.3213, σ_Y= 0.3033; μ_θ= 29°, σ_θ = 9°; L = 71 pixels	μ_Y= 3.2044; σ_Y= 0.5709; μ_θ= 29°, σ_θ = 18°; L = 71 pixels
μ_Y= 3.3623, σ_Y=0.1000; μ_θ= 29 °, σ_θ = 2°; L = 105 pixels	μ_Y= 3.3213, σ_Y= 0.3033; μ_θ= 29°, σ_θ = 9°; L = 105 pixels	μ_Y= 3.2044; σ_Y= 0.5709; μ_θ= 29°, σ_θ = 18°; L = 105 pixels

Appendix： The impact of pore-scale wettability heterogeneity on relative permeability

❑ Results_Impact of SD on relative permeability

- The SD affects the relative permeability of $scCO_2$ more than water. Water flow along surface, insensitive to wettability heterogeneity compared to CO_2.
- The SD affects the relative permeability of $scCO_2$ and water in the middle of saturation axis than ends. When water saturation is in (0.3, 0.7), $scCO_2$ distribution is scattered, resulting uncertainty in relative permeability.

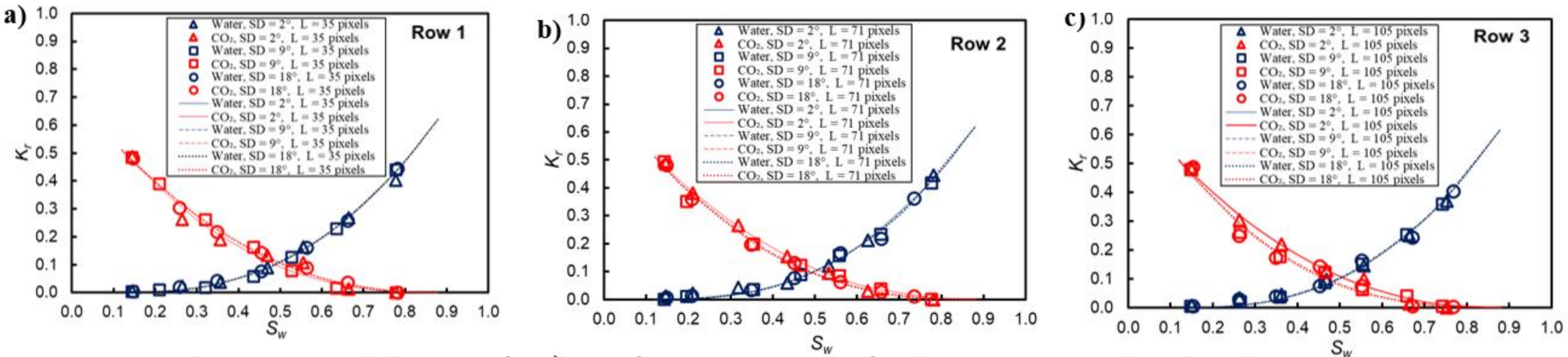

Relative permeability as a function of water saturation for the parameter values listed in (a) row 1, (b) row 2, and (c) row 3 of simulation plan. The scattered data points are simulation measurements. The lines are the Corey model fitting.

❑ Results_Impact of SD on relative permeability

- The “∧” shape relation between *SD* of *kr* and *Sw* clearly demonstrates that impact: $scCO_2$>water, middle > ends.
- Larger *L* leads to larger *SD* of *kr*.

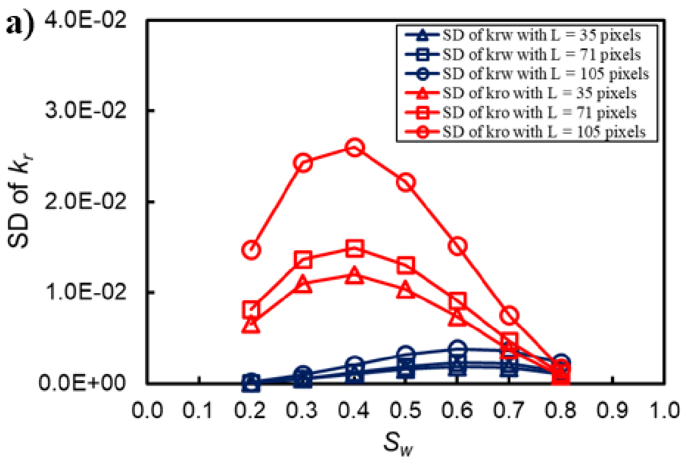

SD between the Corey-model-fitted *kr* values due to the variation in SD of CA as a function of Sw.

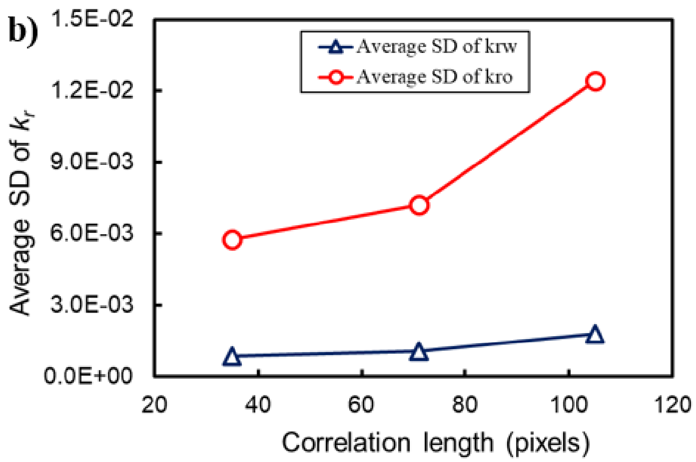

Average SD between the Corey-model-fitted k_r curves as a function of the *L*.

Appendix： The impact of pore-scale wettability heterogeneity on relative permeability

❑ Results_Impact of *L* on CO_2/water configuration

- The *L* affects the relative permeability of scCO_2 more than water. Water flow along surface, insensitive to wettability heterogeneity compared to CO_2.
- The *L* affects the relative permeability of scCO_2 and water in the middle of saturation axis than ends. When water saturation is in (0.3, 0.7), scCO_2 distribution is scattered, resulting uncertainty in relative permeability.

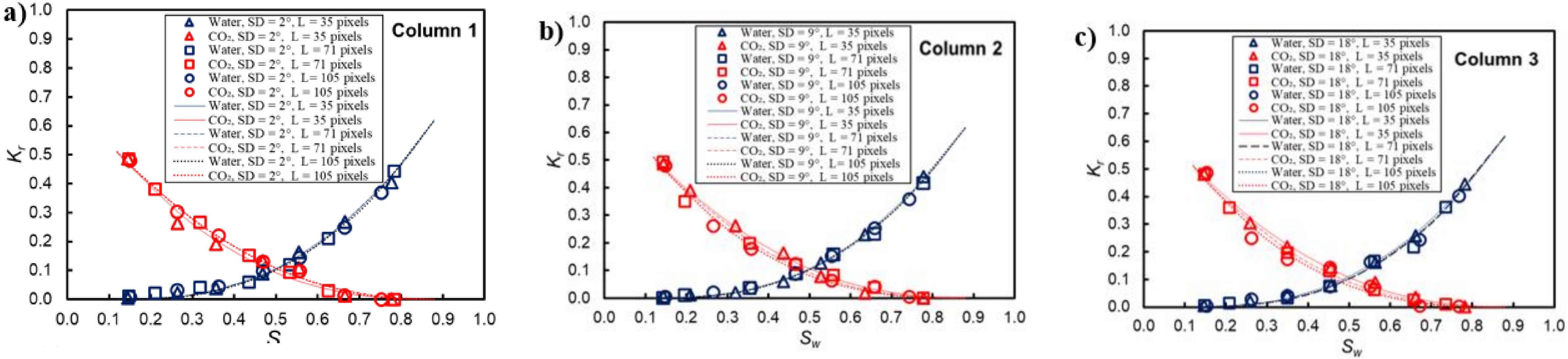

Relative permeability as a function of water saturation for the parameter values listed in (a) column 1, (b) column 2, and (c) column 3 of simulation plan. The scattered data points are simulation measurements. The lines are the Corey model fitting.

Appendix： The impact of pore-scale wettability heterogeneity on relative permeability

❑ Results_Impact of *L* on CO_2/water configuration

- The "Λ" shape relation between *SD* of *kr* and *Sw* clearly demonstrates that impact: $scCO_2$>water, middle > ends.
- Larger *SD* leads to larger *SD* of *kr*.

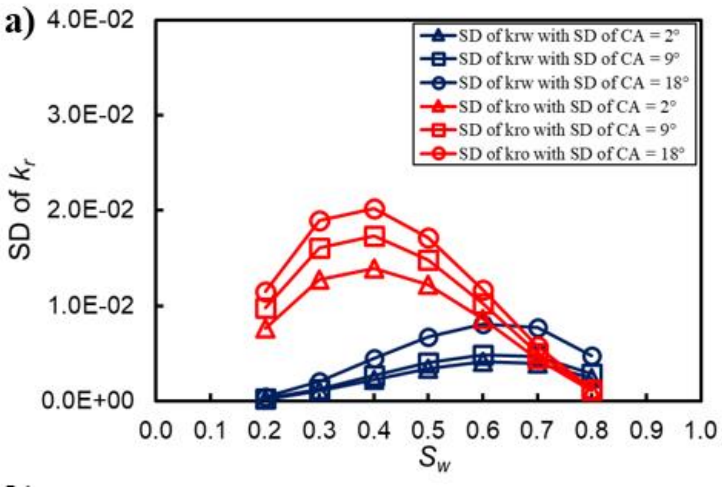

SD between the Corey-model-fitted *kr* values due to the variation in *L* of CA as a function of S_w.

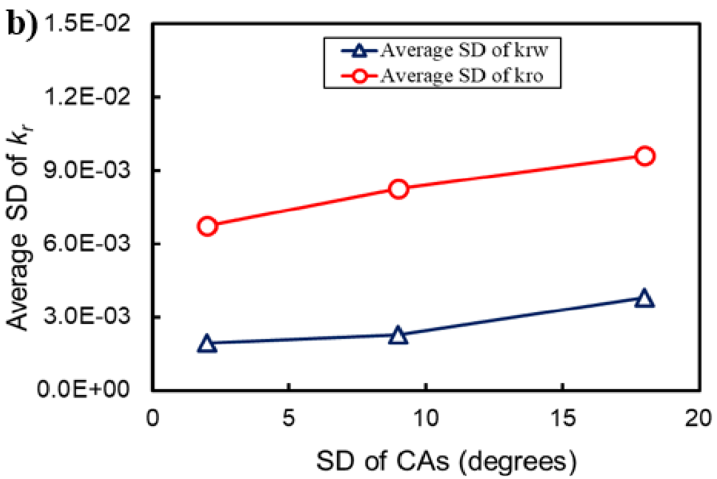

Average *SD* between the Corey-model-fitted k_r curves as a function of the *SD*.